World Journal of Pharmaceutical Science and Research
www.wjpsronline.com
Research Article
ISSN: 2583-6579
SJIF Impact Factor: 5.111
Year - 2024
Volume: 3; Issue: 5
Page: 384-393

FORMULATION AND EVALUATION OF RIFAMPICIN NANOPARTICLES

Kondoju Shailaja and Jimidi Bhaskar*

Department of Pharmaceutics, Bharat Institute of Pharmacy, Mangalpally, Ibrahimpatnam, Ranga Reddy-501510.

Article Received: 08 August 2024 | | ***Article Revised: 27 September 2024*** | | ***Article Accepted: 19 October 2024***

***Corresponding Author: Jimidi Bhaskar**
Department of Pharmaceutics, Bharat Institute of Pharmacy, Mangalpally, Ibrahimpatnam, Ranga Reddy-501510.
DOI: https://doi.org/10.5281/zenodo.14025429

How to cite this Article: Kondoju Shailaja and Jimidi Bhaskar. (2024). FORMULATION AND EVALUATION OF RIFAMPICIN NANOPARTICLES. World Journal of Pharmaceutical Science and Research, 3(5), 384-393. https://doi.org/10.5281/zenodo.14025429

ABSTRACT

Nanoparticles offer innovative solutions for drug delivery and research due to their unique size-dependent properties and potential for new therapeutic developments. They enable controlled and site-specific drug delivery, presenting advantages over traditional vehicles like creams and emulsions, such as controlled release, minimal skin irritation, and active compound protection. However, challenges include drug expulsion from nanoparticles due to the highly ordered crystalline lipid matrix, which restricts drug accommodation. To address this, nanostructured lipid carriers (NLC) were explored. This study focuses on formulating Rifampicin nanoparticles using NLC to enhance stability and targeted delivery. Rifampicin, an antimicrobial agent for mycobacterial and gram-positive infections, was chosen as the model drug. The research evaluates the performance of Rifampicin-loaded NLC in terms of drug release, stability, and efficacy, demonstrating significant improvements in drug delivery systems.

KEYWORDS: Nanostructured Lipid carriers (NLC), Nanotechnology, Nanoparticles.

1. INTRODUCTION

Nanotechnology, focusing on particles between 1 and 100 nanometres, has garnered significant attention due to the unique properties of nanoparticles at this scale. These particles, composed of materials like carbon, metals, or organic compounds, exhibit distinct physical, chemical, and biological behaviours compared to larger particles, attributed to their high surface-area-to-volume ratio and enhanced reactivity or stability. Nanoparticles come in various shapes and sizes, including zero-dimensional nano dots, one-dimensional structures like graphene, two-dimensional forms such as carbon nanotubes, and three-dimensional entities like gold nanoparticles. They can be spherical, cylindrical, conical, or irregular, with diverse surface characteristics and structural forms. Advances in synthesis methods and instrumentation have improved nanoparticle properties and reduced production costs, leading to their integration into a wide range of applications from cooking utensils and electronics to renewable energy and aerospace, highlighting their role in advancing sustainable technologies.[1-5]

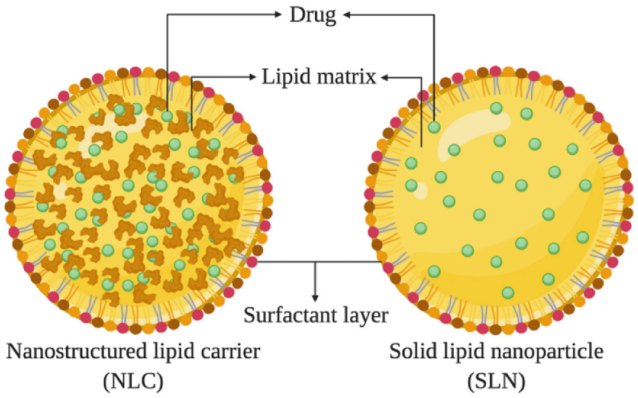

Figure-1: Comparative illustration of Nanostructured Lipid Carriers (NLC) and Solid Lipid Nanoparticles (SLN) showcasing their structural differences and drug incorporation capacities.

Various methods have been developed for nanoparticle preparation, each offering distinct advantages and limitations. The solvent evaporation method involves preparing a nano emulsion by dissolving the polymer in an organic solvent and dispersing it with a drug, which is then emulsified in an aqueous phase containing surfactants. Following emulsion formation, the organic solvent is evaporated under reduced pressure. The double emulsification method addresses the challenge of hydrophilic drug entrapment by first creating a water-in-oil (w/o) emulsion and then further emulsifying it into a water-in-oil-in-water (w/o/w) emulsion, with solvent removal achieved by high centrifugation. The emulsions-diffusion method, a variation of the salting-out technique, uses water-miscible solvents and saturates them with water to create stable emulsions, benefiting from high encapsulation efficiencies and reproducibility but requiring extensive water removal. Nano precipitation, or solvent displacement, involves dissolving the drug and polymer in an organic solvent and then diffusing this solution into an aqueous medium. The coacervation method, involving ionic gelation, uses biodegradable polymers to form nanoparticles through electrostatic interactions, followed by cross-linking and purification. The salting-out method separates water-miscible solvents from aqueous solutions using salting-out agents, which promotes nanoparticle formation without high temperatures. Finally, dialysis involves dissolving the polymer and drug in an organic solvent and performing dialysis against a non-solvent, leading to nanoparticle formation through solvent displacement. Each method offers unique benefits for nanoparticle production, from improved encapsulation and stability to ease of scaling up. While nanoparticles offer significant advantages for controlled and targeted drug delivery, including enhanced drug stability, they also present some limitations. A key issue observed during storage is the expulsion of the drug from nanoparticles, attributed to the highly ordered crystalline lipid matrix which limits available space for drug molecules. To address this challenge, nanostructured lipid carriers (NLCs) have been developed. In this study, rifampicin, an antimicrobial drug used to treat various mycobacterial and gram-positive infections, has been chosen as the model drug to evaluate the effectiveness of NLCs in improving drug delivery and stability.[6-10]

2. EXPERIMENTAL

2.1. Materials

Eudragit RS100 was a gift sample from Seeko Biotech, Vijayawada, Andhra Pradesh. Rifampicin (Himedia laboratories, Nasik), Chitosan, Ethyl cellulose, Dichloromethane, Tween 80, Span 60, Methanol was produced from commercial sources. All other materials were of pharmacopoeial grade.

2.2. Methods

A. Analytical method development

To determine the absorption maxima of Rifampicin, a stock solution was prepared by dissolving 100 mg of the drug in 100 mL of methanol (1 mg/mL). From this, 1 mL was diluted to 100 mL with phosphate buffer (pH 5.5), and further dilution (1 mL to 10 mL) was performed for UV scanning in the 200-400 nm range using a double-beam UV spectrophotometer. The absorption maxima were identified at 279 nm. For the calibration curve, Rifampicin was dissolved in methanol, and a stock solution (1 mg/mL) was prepared. Working standards (5, 10, 15, 20, and 25 µg/mL) were made by dilution with phosphate buffer (pH 5.5) and analyzed using the UV method. The process was repeated thrice, with the average peak area calculated. A calibration plot was then constructed between concentration and peak area, and the calibration equation along with the R^2 value were recorded.[11-16]

B. Preparation of Rifampicin loaded nanoparticles

Rifampicin-loaded nanoparticles were prepared using the emulsification-sonication method. Rifampicin was dissolved in a mixture of methanol (15 mL) and dichloromethane (20 mL). Polymers, at varying concentrations, were dissolved in water, and the organic phase was added dropwise to the polymer solution for emulsification. The dispersion was then sonicated for 20 minutes using an ultra-probe sonicator (60 W/cm³, Hielscher, Germany) and stirred at 1500 rpm for 6 hours to evaporate the organic solvent. The nanoparticles were centrifuged at 15,000 rpm for 20 minutes at 25°C, separated, lyophilized with 0.2% mannitol as a cryoprotectant, and stored for further evaluation.

Table-1: Composition of Rifampicin Nanoparticle formulation (R1-R9).

Excipients	R1	R2	R3	R4	R5	R6	R7	R8	R9
Rifampicin (mg)	50	50	50	50	50	50	50	50	50
Eudragit RS 100 (mg)	25	50	75	-	-	-	-	-	-
Chitosan (mg)	-	-	-	25	50	75	-	-	-
Ethyl cellulose	-	-	-	-	-	-	25	50	75
Tween 80 (mL)	1	1.5	2	2.5	-	-	-	-	1
Span 60 (mL)	-	-	-	-	1	1.5	2	2.5	1
Distilled water (ml)	Q.S	Q.S	Q.S	Q.S	Q.S	Q.S	Q.S	Q.S	Q.S
Dichloromethane (ml)	20	20	20	20	20	20	20	20	20
Methanol	15	15	15	15	15	15	15	15	15

C. Characterization of Nanoparticles

The mean particle size and polydispersity index (PDI), which indicates the distribution of nanoparticle populations, were determined using dynamic light scattering (Delta Nano C, Beckman Counter), while the zeta potential was estimated based on electrophoretic mobility in an electric field, using a Zeta Sizer Nano ZS (Malvern Instruments, UK). Prior to measurement, samples were diluted with distilled water and analyzed at a fixed angle of 165° for particle size and PDI. For zeta potential analysis, samples were diluted at a 1:40 ratio with filtered water (v/v). All measurements for average particle size, PDI, and zeta potential were conducted in triplicate. To determine the drug content of Rifampicin in solid lipid nanoparticles, 100 mg of nanoparticles were dissolved in 10 ml methanol, followed by shaking for 5 minutes. A 1 ml aliquot of the resulting solution was further diluted to 10 ml with methanol, and absorbance was measured at 279 nm using a UV-visible spectrophotometer (Lab India 3200).[17-25]

Yield of nanoparticles: The yield of solid lipid nanoparticles was calculated using the formula

$$Percentage\ yield = \frac{Total\ weight\ of\ nanoparticles}{Total\ weight\ of\ drug\ +\ weight\ of\ added\ materials} \times 100$$

Entrapment Efficiency: Entrapment efficiency (EE) of Rifampicin-loaded nanoparticles was determined by measuring the concentration of unentrapped drug in an aqueous medium using the centrifugation method. The nanoparticles were centrifuged at 5000 rpm for 15 minutes at 4°C in a high-speed cooling centrifuge (C-24, Remi), utilizing Nano step centrifuge tubes with an ultrafilter having a molecular mass cutoff of 100 kDa (Pall Life Sciences, India). The supernatant was then separated, and the amount of Rifampicin in the supernatant was quantified using a UV-Visible spectrophotometer (U-1800, Hitachi) at a wavelength of 279 nm after appropriate dilution. The percentage of entrapment efficiency was calculated using the following formula:

$$\% EE = \frac{Total\ drug\ content - Free\ drug}{Total\ drug\ content} \times 100$$

D. *In-Vitro* Drug release

In vitro drug release studies were conducted in simulated gastric fluid (SGF, pH 1.2) and simulated intestinal fluid (SIF, pH 7.4), prepared according to the United States Pharmacopoeia, at 37°C under shaking conditions. At predetermined intervals, aliquots were withdrawn and replaced with an equal volume of fresh buffer. The rifampicin-loaded nanoparticles were separated from the aqueous suspension by ultracentrifugation at 10,000 rpm for 10 minutes using a SORALL® Bioguge Stratos Ultracentrifuge. The concentration of rifampicin was measured by absorbance at 475 nm using a UV-visible spectrophotometer (Perkin Elmer Lambda Bio 40). Data are presented as mean ± standard deviation (SD) from nine independent measurements.[26]

E. Drug release kinetics

Data of *in vitro* release studies of formulations which were showing better drug release were fit into different equations to explain the release kinetics of drug release from Nanoparticles. The data was fitted into various kinetic models such as zero, first order kinetics; higuchi and korsmeyer peppas mechanisms.

F. SEM (Scanning Electron microscope) studies

The surface morphology of the layered sample was examined using SEM (Hitachi, Japan). A small amount of powder was manually dispersed onto a carbon-coated aluminum stub, then coated with a thin 30 A^o layer of gold using a POLARON-E 3000 sputter coater. The samples were imaged at various magnifications, with the images directly captured onto a computer.

G. Powder X-ray Diffraction (PXRD) Studies

The prepared mixtures were analyzed using X-ray powder diffraction (PXRD) to confirm the formation of new solid phases. Differences in 2 theta lines indicated the creation of new solid phases, as no two solids share identical 2 theta patterns. PXRD provided insights into the crystal structure, chemical composition, and physical properties, making it a valuable tool for studying polymorphism, pharmaceutical salts, and cocrystalline phases. The samples were scanned from 10° to 40° 2θ using nickel-filtered CuKα radiation (40 kV, 30 mA) on a sample stage Spinner PW3064 with a step size of 0.045° and a step time of 0.5 seconds.[27-30]

3. RESULTS AND DISCUSSION

3.1. Determination of Absorption Maxima and Calibration Curve

The absorption maxima of Rifampicin were determined using spectrophotometry, with the maximum absorption observed at 279 nm. Subsequently, a calibration curve for Rifampicin was constructed using measurements taken in

phosphate buffer at pH 7.4. The standard graph of Rifampicin showed good linearity with R^2 of 0.999, which indicates that it obeys “Beer- Lamberts” law.

Table-2: Calibration curve data for Rifampicin at 279nm.

Concentration [µg/mL]	Absorbance (279 nm)
0	0
5	0.117
10	0.236
15	0.351
20	0.463
25	0.587

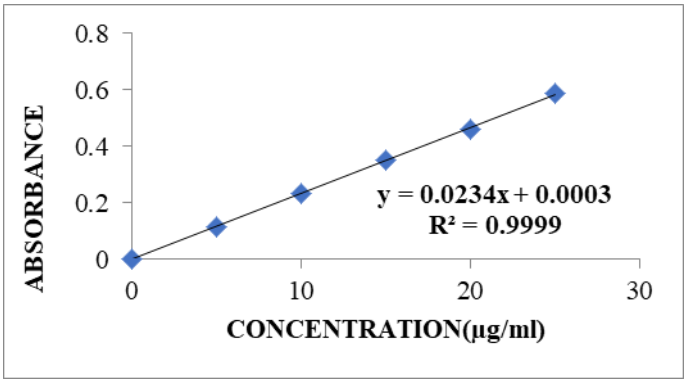

Figure-2: Standard graph of Rifampicin in 7.4 Phosphate buffer.

3.2. Evaluation of Rifampicin Loaded Nanoparticles

The evaluation of Rifampicin-loaded nanoparticles involved assessing various parameters for all nine formulations, including Mean Particle Size, Percentage Yield, Drug Content, Drug Encapsulation Efficiency, Polydispersity Index (PDI), and Zeta Potential. These metrics provide comprehensive insights into the nanoparticles' characteristics and performance. Detailed results for these parameters are summarized in the Table-3. Percentage yield of formulations R1 to R9 by varying drug was determined and is presented in Table-3. Highest drug content, Highest Entrapment efficiency observed for R5 formulation. PDI observed in the R5 formulation i.e., 0.309 respectively. The Zeta potential range from -25.72 mV to -33.64 mV to all the formulations.

Table-3: Evaluation of Nanoparticles.

Formulation Code	Mean Particle size(nm)	% Yield	Drug Content	Drug encapsulation efficiency	PDI	Zeta Potential (mV)
R1	286.21± 18	78.41	93.51	74.92	0.668	-27.13± 1.8
R2	291.22 ± 19	61.64	95.81	82.29	1.278	-29.22 ± 1.9
R3	301.19 ± 16	72.82	97.65	79.41	1.164	-31.18 ± 1.6
R4	256.22 ± 20	65.30	91.54	77.91	0.888	-26.23 ± 2.0
R5	267.56± 18	69.91	94.82	83.83	0.576	-29.57± 1.8
R6	271.72± 23	76.44	98.84	88.92	0.301	-33.64± 2.3
R7	341.72± 23	83.82	95.41	74.92	0.499	-26.71± 2.3
R8	358.32± 42	87.79	97.14	82.29	0.372	-27.36± 2.2
R9	361.52± 32	93.54	97.28	79.41	0.336	-28.58± 2.4

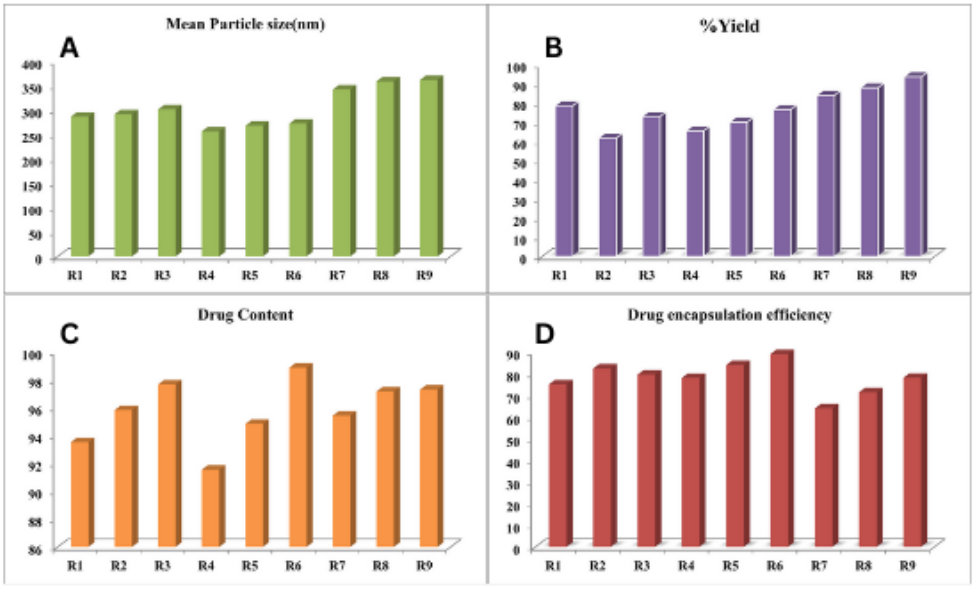

Figure-3: Graphical representation of A- Mean Particle size (nm); B- %Yield; C- Drug content; D- Drug encapsulation efficiency.

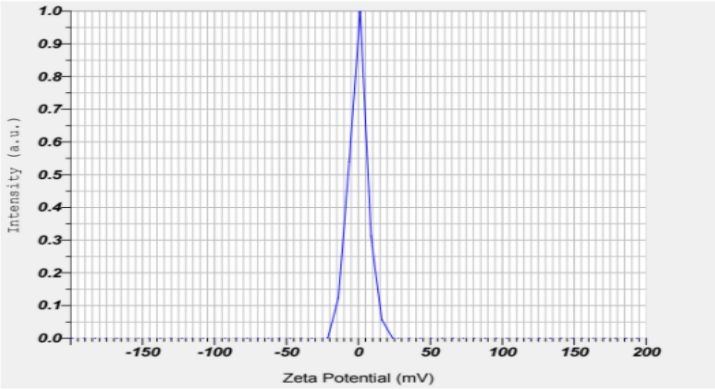

Figure-4: Zeta potential of R5 formulation.

3.3. *In-Vitro* release studies

Table-4: *In vitro* Drug release studies of Rifampicin loaded Nanoparticles.

Time (hr)	R1	R2	R3	R4	R5	R6	R7	R8	R9
0	0	0	0	0	0	0	0	0	0
1	12.24	24.69	22.14	17.3	17.58	12.62	21.29	18.29	13.11
2	24.93	41.09	37.96	31.26	25.67	22.87	32.63	22.56	19.82
3	37.06	44.61	52.43	48.21	32.05	31.63	43.16	34.98	32.15
4	46.15	56.56	61.16	51.74	48.11	47.32	56.35	45.23	42.89
5	57.26	62.91	72.82	61.58	52.87	56.89	64.88	53.78	55.13
6	68.73	75.22	77.93	75.86	69.98	67.64	73.64	66.09	61.75
7	75.62	79.67	82.65	81.93	73.34	75.86	82.78	74.63	68.04
8	86.87	84.45	89.89	85.77	87.41	83.41	87.92	78.77	76.19
10	89.28	91.43	91.81	91.12	94.25	92.31	92.41	91.35	84.42
12	92.33	94.19	96.41	97.08	99.17	97.37	95.49	97.19	94.34

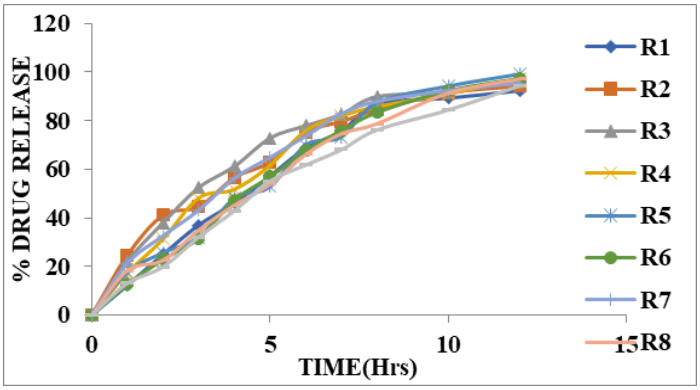

Figure-5: Graphical representation of dissolution study of Rifampicin Nanoparticles.

Based on dissolution data, the R5 Chitosan (1:2) (50 mg) formulation demonstrated the best release (99.17%) over 12 hours, making it the optimized formulation.

3.4. Drug release kinetics

Table-5: Release kinetics data for optimized formulation (R5).

Cumulative (%) Release	Time (T)	Root (T)	Log (%) Release	Log (T)	Log (%) Remain	Release Rate	1/Cum% release	Peppas Log Q/100	% drug Remain	Q01/3	Q01/3	Q01/3-Q01/3
0	0	0			2.000				100	4.642	4.642	0.000
17.5	1	1.000	1.245	0.000	1.916	17.580	0.0569	-0.755	82.42	4.642	4.352	0.290
25.67	2	1.414	1.409	0.301	1.871	12.835	0.0390	-0.591	74.33	4.642	4.205	0.437
32.05	3	1.732	1.506	0.477	1.832	10.683	0.0312	-0.494	67.95	4.642	4.081	0.561
48.11	4	2.000	1.682	0.602	1.715	12.028	0.0208	-0.318	51.89	4.642	3.730	0.912
52.87	5	2.236	1.723	0.699	1.673	10.574	0.0189	-0.277	47.13	4.642	3.612	1.029
69.98	6	2.449	1.845	0.778	1.477	11.663	0.0143	-0.155	30.02	4.642	3.108	1.534
73.34	7	2.646	1.865	0.845	1.426	10.477	0.0136	-0.135	26.66	4.642	2.987	1.654
87.41	8	2.828	1.942	0.903	1.100	10.926	0.0114	-0.058	12.59	4.642	2.326	2.315
94.25	10	3.162	1.974	1.000	0.760	9.425	0.0106	-0.026	5.75	4.642	1.792	2.850
99.17	12	3.464	1.996	1.079	-0.081	8.264	0.0101	-0.004	0.83	4.642	0.940	3.702

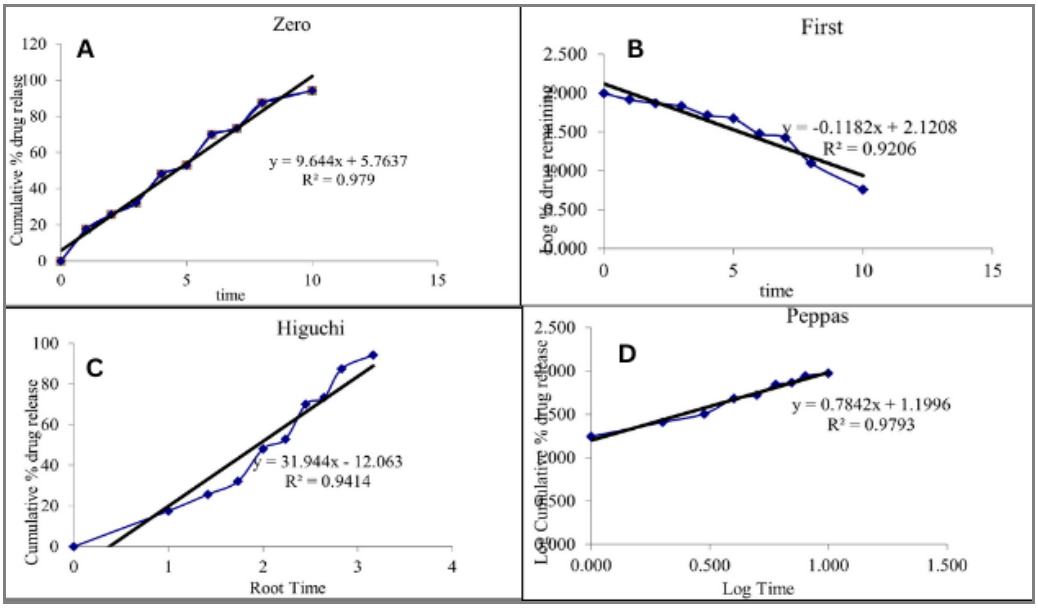

Figure-6: Graphs showing A- zero order kinetics; B- first order release kinetics; C- higuchi release kinetics; D- peppas release kinetics. Based on the data above results the optimized formulation followed *first order* release kinetics.

3.5. SEM (Scanning Electron microscope) studies

SEM studies showed that the Rifampicin - loaded nanoparticles had a spherical shape with a smooth surface as shown in Figure-7.

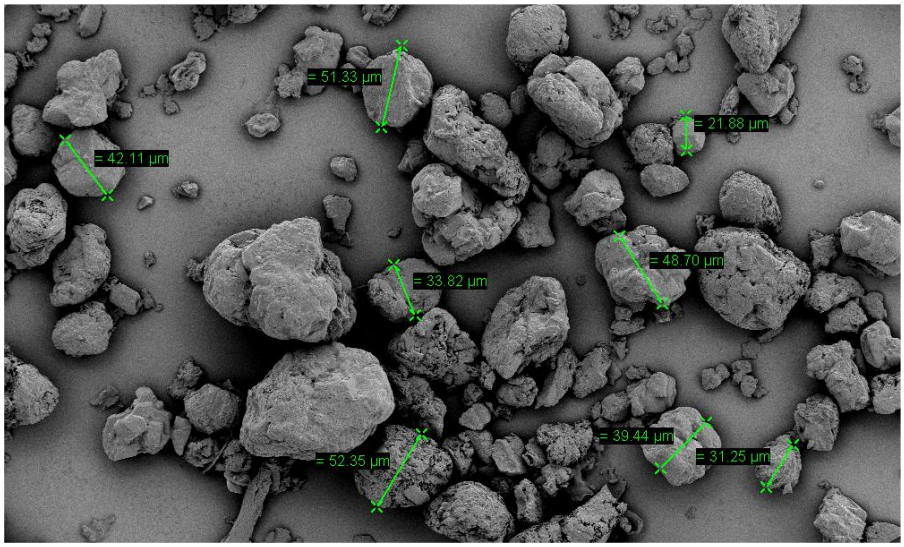

Figure-7: SEM graph of optimized formulation.

3.6. Powder X-ray Diffraction (PXRD) Studies

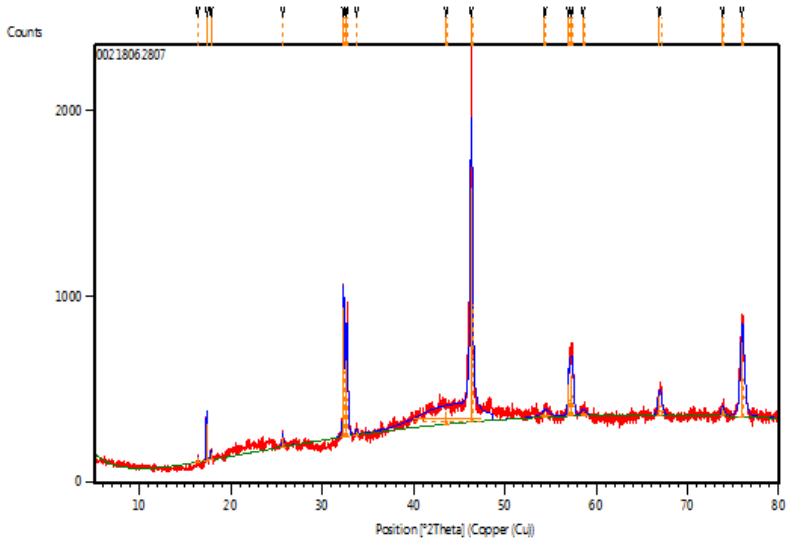

Figure-8: XRD study of Rifampicin loaded nanoparticle R5 optimised formulation.

CONCLUSION

The primary objective of this study was to formulate and evaluate Rifampicin nanoparticles utilizing various polymers, including Eudragit RS 100, Chitosan, and Ethyl Cellulose in different ratios. In vitro drug release studies demonstrated that the formulation R5, which incorporates a combination of these polymers, achieved an impressive drug release of over 99.17% over a 12-hour period. This formulation has been identified as the optimized variant, showing significant promise for sustained drug delivery. Fourier-transform infrared (FT-IR) spectroscopy confirmed the absence of any drug-excipient interactions in the optimized formulation. Based on these results, formulation R5 stands out as a

potentially effective sustained-release system for Rifampicin, offering nearly zero-order release kinetics and thereby improving patient compliance through prolonged therapeutic effects. Further in vivo studies are recommended to validate the clinical efficacy and optimize patient outcomes.

REFERENCES

1. Hasan S. A review on nanoparticles: their synthesis and types biosynthesis: mechanism, 2015; 4: 9–11.
2. Bundschuh M, Filser J, Lüderwald S, McKee MS, Metreveli G, Schaumann GE, Schulz R, Wagner S. Nanoparticles in the environment: where do we come from, where do we go to? Environmental Sciences Europe, 2018 Dec; 30: 1-7.
3. Cho EJ, Holback H, Liu KC, Abouelmagd SA, Park J, Yeo Y. Nanoparticle characterization: state of the art, challenges, and emerging technologies, 2013.
4. Machado S, Pacheco JG, Nouws HPA, Albergaria JT, Delerue-Matos C. Characterization of green zero-valent iron nanoparticles produced with tree leaf extracts. Sci Total Environ, 2015; 533: 76–81.
5. Tiruwa R. A review on nanoparticles – preparation and evaluation parameters. Indian J Pharm Biol Res, 2015; 4(2): 27–31.
6. Abhilash M. Potential applications of nanoparticles. Int J Pharma Bio Sci, 2010; 1(1): 1–12.
7. Nagavarma BVN, Hemant KS, Ayuz A, Vasudha LS, Shivakumar HG. Different techniques for preparation of polymeric nanoparticles – a review. Asian J Pharm Clin Res, 2012; 5(3): 1–8.
8. Mullaicharam AR. Nanoparticles in drug delivery system. Int J Nutr Pharmacol Neurol Dis, 2011; 1(2): 103–121.
9. Langer R. Biomaterials in drug delivery and tissue engineering: one laboratory's experience. Acc Chem Res, 2000; 33: 94–101.
10. Bhadia D, Bhadra S, Jain P, Jain NK. Pegnology: a review of PEGylated systems. Pharmazie, 2002; 57(5–20).
11. Tiwari DK, Behari J, Sen P. Application of nanoparticles in wastewater treatment, 2008; 3: 417–33.
12. Salavati-Niasari M, Davar F, Mir N. Synthesis and characterization of metallic copper nanoparticles via thermal decomposition. Polyhedron, 2008; 27: 3514–8.
13. Tai CY, Tai C, Chang M, Liu H. Synthesis of magnesium hydroxide and oxide nanoparticles using a spinning disk reactor, 2007; 5536–41.
14. Bhaviripudi S, Mile E, Shah SA, Zare AT, Dresselhaus MS, Belcher AM, et al. CVD synthesis of single-walled carbon nanotubes from gold nanoparticle catalysts, 2007; 1516–7.
15. Allouche J. Synthesis of organic and bioorganic nanoparticles: an overview of the preparation methods. Springer-Verlag London, 2013; 27–30.
16. Tamizhrasi S, Shukla A, Shivkumar T, Rathi V, Rathi JC. Formulation and evaluation of lamivudine-loaded polymethacrylic acid nanoparticles. Int J PharmTech Res, 2009; 1(3): 411–5.
17. Mohanraj VJ, Chen Y. Nanoparticles – a review. Trop J Pharm Res, 2006; 5(1): 561–73.
18. Das S, Banerjee R, Bellare J. Aspirin-loaded albumin nanoparticles by coacervation: implications in drug delivery. Trends Biomater Artif Organs, 2005; 18(2): 1–10.
19. Chokshi NV, Rawal S, Solanki D, Gajjar S, Bora V, Patel BM, et al. Fabrication and characterization of surface-engineered rifampicin-loaded lipid nanoparticulate systems for the potential treatment of tuberculosis. J Pharm Sci., 2021; 110(5): 2221–32.
20. Prabhu P, Fernandes T, Chaubey P, Kaur P, Narayanan S, VK R, et al. Mannose-conjugated chitosan nanoparticles for delivery of rifampicin to osteoarticular tuberculosis. Drug Deliv Transl Res, 2019; 11: 1509.

21. Gardouh A, Gamal A, Gad S. Formulation and pharmacokinetic evaluation of rifampicin solid lipid nanoparticles. J Res Pharm.
22. Design and Evaluation of Moxifloxacin microbeads by covalent crosslinking method. International Journal of Chemistry and Pharmaceutical Sciences, 2018; 6(8): 221-227.
23. Scolari IR, Páez PL, Sánchez-Borzone ME, Granero GE. Promising chitosan-coated alginate-tween 80 nanoparticles as rifampicin coadministered ascorbic acid delivery carrier against Mycobacterium tuberculosis. AAPS PharmSciTech, 2019; 2: 67.
24. Rani S, Gothwal A, Pandey PK, Chauhan DS, Pachouri PK, Gupta UD, et al. HPMA-PLGA based nanoparticles for effective in vitro delivery of rifampicin. Pharm Res, 2019; 36(19).
25. Chokshi NV, Khatri HN, Patel MM. Formulation, optimization, and characterization of rifampicin-loaded solid lipid nanoparticles for the treatment of tuberculosis. Drug Dev Ind Pharm, 2018; 44(12): 1975–89.
26. Sheaikh SS, Harkal SK, Gaikwad RP, Gawali RW, Deshmukh DP. Formulation and evaluation of polymeric nanoparticles of rifampicin for antitubercular therapy. Int J Healthc Med Sci, 2018; 4(6): 117–22.
27. Vieira ACC, Magalhães J, Rocha S, Cardoso MS, Santos SG, Borges M. Targeted macrophage delivery of rifampicin-loaded lipid nanoparticles to improve tuberculosis treatment. Nanomedicine, 2017; 12(24).
28. Parmar R, Misra R, Mohanty S. In vitro controlled release of rifampicin through liquid-crystalline folate nanoparticles. Colloids Surf B Biointerfaces, 2015; 129: 198–205.
29. Mohseni M, Gilani K, Bahrami Z, Bolourchian N, Mortazavi SA. Preparation and in-vitro evaluation of rifampin-loaded mesoporous silica nanoaggregates by an experimental design. Iran J Pharm Res, 2015; 14(2): 359–71.
30. Preparation and characterisation of Mucoadhesive microspheres containing clopidogrel - The Pharmainnovation Journal, 2013; 2(2): 15-22.